Computer Assisted Mechanics and Engineering Sciences, 7: 69–80, 2000.

Semi-analytical sensitivity analysis procedure for frictional contact problems

Xian Chen, Toshiaki Hisada
Department of Environmental Studies, Graduate School of Frontier Sciences, The University of Tokyo, 7-3-1 Hongo, Bunkyo-Ku, Tokyo, 113-0033, Japan

Kazuhiro Nakamura, Masahiko Mori
Takasago R&D Center, Mitsubishi Heavy Industries, Ltd. 2-1-1, Shinhama Arai-Cho, Takasago, Hyogo Pref. 676-8686, Japan

(Received May 20, 1999)

Although there is a need for sensitivity analysis for frictional contact problems in many engineering fields, research work on it has rarely been reported due to the complexity of the problems. In this paper, a sensitivity analysis procedure based on a semi-analytical method for frictional contact problems is presented. The unbalance force due to the variation of design parameters is evaluated numerically, thus the related routine of an existing FEM code can be utilized regardless of the friction law employed. The continuum-mechanics-based formulation is carried out first and then a discretized form is derived. The stick state is modeled by introducing a penalty-type constraint. A couple of numerical examples, including a realistic leaf spring structure used in nuclear power plants, are given to demonstrate the effectiveness of the proposed approach.

1. Introduction

The purpose of sensitivity analysis is to determine the gradients, i.e., sensitivities, of structural response with respect to design parameters. In manufacturing, sensitivity analysis is introduced to indicate the influence of design parameters on product quality, or to reveal the dominant factors to aid troubleshooting. In addition, with the significant progress of advanced design, the need for sensitivity analysis is increasing in many fields, such as design optimization and structural reliability analysis. The most direct method of sensitivity analysis is the finite difference method (FDM). In this method, finite element analysis is carried out on the design and the perturbed values of each design parameter, then the sensitivities are computed from the differences in the results of the finite element analysis. However, for large-scale problems with many design parameters, this method may become inefficient due to the long CPU time required and the high cost of computation. The research on efficient sensitivity analysis methods of linear and path-independent nonlinear problems has reached maturity [7]. In recent years, sensitivity analysis methods have been extensively developed for various nonlinear problems. In particular, for path-dependent problems, the direct differentiation method (DDM), in which the formulation is carried out by strictly differentiating the basic equations, is now mainly adopted from the viewpoint of computational efficiency [9, 12, 13].

On the other hand, due to the nonlinearity resulting from boundary changes, the analytical solution of frictional contact problems is usually difficult to obtain and hence finite element analysis plays an important role [14, 15]. In contrast to the development of finite element analysis, the sensitivity analysis of frictional contact problems seems to remain almost unexplored. Kleiber and his coworkers presented a sensitivity analysis algorithm for unilateral frictional contact problems and applied it to metal forming processes [1, 2, 10]. In the paper by Pollock and Noor [11], a sensitivity

analysis method was presented for frictional contact/impact between a composite shell structure and a flat rigid surface. The DDM procedure was adopted in those works. On the other hand, the authors [5] have proposed a sensitivity analysis approach for elastoplastic frictionless contact problems with large deformation, by using the semi-analytical differentiation method (SDM). In this work, for frictional contact problems, a general approach of sensitivity analysis based on SDM is proposed. The formulation starts from the differentiation of basic equations, as in the DDM, but the variations in internal force, friction and contact forces are evaluated numerically with respect to the design parameters. Thus, by using the subroutine of the existing finite element analysis code with minimal code modification, no special attention need be paid to the concrete forms of the constitutive and friction laws. Furthermore, the computational efficiency of DDM can be maintained, i.e., sensitivity analysis can be performed at the same time as the finite element analysis but without iteration.

2. Sensitivity analysis formulation

2.1. Finite element analysis for frictional contact problems with large deformation

As a preparation for sensitivity analysis, the finite element analysis approach for frictional contact problems is introduced in this section. The total Lagrangian formulation is used to describe large deformation. Fig. 1 shows the surfaces of body 1 and body 2. The hitting point $\boldsymbol{x}^h$ of body 2 is

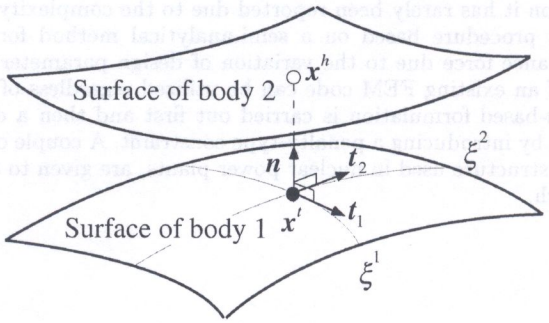

Fig. 1. Contact surfaces

going to contact the target point $\boldsymbol{x}^t$, which is the projection of $\boldsymbol{x}^h$ onto the surface of body 1. The superscripts h and t represent the hitting and target points, respectively. Denoting the convected coordinates of $\boldsymbol{x}^t$ as ξ^1 and ξ^2, the covariant base vectors $\boldsymbol{t}_1$ and $\boldsymbol{t}_2$ and the outer normal unit vector $\boldsymbol{n}$ are given as

$$\boldsymbol{t}_1 = \frac{\partial \boldsymbol{x}^t}{\partial \xi^1}, \qquad \boldsymbol{t}_2 = \frac{\partial \boldsymbol{x}^t}{\partial \xi^2}, \qquad \boldsymbol{n} = \frac{\boldsymbol{t}_1 \times \boldsymbol{t}_2}{|\boldsymbol{t}_1 \times \boldsymbol{t}_2|}. \tag{1}$$

For the contacting bodies in an equilibrium state, forces acting at contact points $\boldsymbol{x}^t$ and $\boldsymbol{x}^h$, denoted by $\boldsymbol{p}^t$ and $\boldsymbol{p}^h$, can be decomposed into contact forces (normal components) $\boldsymbol{p}_n^t$, $\boldsymbol{p}_n^h$ and friction forces (tangential components) $\boldsymbol{p}_t^t$, $\boldsymbol{p}_t^h$. Then the relations

$$\boldsymbol{p}^t = \boldsymbol{p}_n^t + \boldsymbol{p}_t^t, \qquad \boldsymbol{p}^h = \boldsymbol{p}_n^h + \boldsymbol{p}_t^h, \tag{2}$$

$$\boldsymbol{p}_n \equiv \boldsymbol{p}_n^t = -\boldsymbol{p}_n^h, \qquad \boldsymbol{p}_t \equiv \boldsymbol{p}_t^t = -\boldsymbol{p}_t^h, \tag{3}$$

$$\gamma_c \equiv \gamma_c^1 = \gamma_c^2, \tag{4}$$

hold where γ_c^1 and γ_c^2 are contact areas of body 1 and body 2. Using the above relations and representing contact and friction forces as

$$\boldsymbol{p}_n = p_n \boldsymbol{n}, \qquad \boldsymbol{p}_t = p_t^i \boldsymbol{t}_i, \tag{5}$$

the virtual work on contact surfaces is given by

$$W = \int_{\gamma_c^1} \boldsymbol{p}^t \cdot \delta \boldsymbol{u}^t \, \mathrm{d}s + \int_{\gamma_c^2} \boldsymbol{p}^h \cdot \delta \boldsymbol{u}^h \, \mathrm{d}s \quad = \int_{\gamma_c} \left[p_n \boldsymbol{n} \cdot (\delta \boldsymbol{u}^t - \delta \boldsymbol{u}^h) + p_t^i \boldsymbol{t}_i \cdot (\delta \boldsymbol{u}^t - \delta \boldsymbol{u}^h) \right] \mathrm{d}s, \tag{6}$$

where the summation convention has been used for the convected coordinate system. On the other hand, defining vector $\boldsymbol{g}$ as

$$\boldsymbol{g} \equiv \boldsymbol{x}^t - \boldsymbol{x}^h \tag{7}$$

gives the penetration

$$g = \boldsymbol{g} \cdot \boldsymbol{n} \tag{8}$$

and

$$\boldsymbol{t}_i \cdot \boldsymbol{g} = 0 \qquad (i = 1, 2). \tag{9}$$

From the definition of target point $\boldsymbol{x}^t$, it is noted that the motion of $\boldsymbol{x}^t$ depends not only on the deformation of body 2 but also on the motion of hitting point $\boldsymbol{x}^h$. Then the variations of Eqs. (7) and (9) give

$$\delta \boldsymbol{g} = \boldsymbol{t}_i \, \delta \xi^i + \delta \boldsymbol{u}^t - \delta \boldsymbol{u}^h, \tag{10}$$

$$\delta \boldsymbol{t}_i \cdot (\boldsymbol{x}^t - \boldsymbol{x}^h) + (\boldsymbol{t}_i \cdot \boldsymbol{t}_j) \, \delta \xi^j + \boldsymbol{t}_i \cdot (\delta \boldsymbol{u}^t - \delta \boldsymbol{u}^h) = 0 \qquad (i = 1, 2). \tag{11}$$

By considering the normality of the normal vector to the covariant base vectors, together with the relation of $\boldsymbol{g} = \boldsymbol{0}$ in the equilibrium state and the relation between the covariant and contravariant components of the friction force vector, Eq. (6) can be rewritten as

$$W = \int_{\gamma_c} \left[p_n \boldsymbol{n} \cdot \delta \boldsymbol{g} - p_{tj} \, \delta \xi^j \right] \mathrm{d}s. \tag{12}$$

Thus, by using the total Lagrangian formulation, the virtual work equation for the structure and the constraint condition in a weak form are given by

$$\int_{\Omega} \boldsymbol{S} : \delta \boldsymbol{E} \, \mathrm{d}V = \int_{\Gamma} \bar{\boldsymbol{t}} \cdot \delta \boldsymbol{u} \, \mathrm{d}S + \int_{\Omega} \rho_0 \boldsymbol{g} \cdot \delta \boldsymbol{u} \, \mathrm{d}V + \int_{\Gamma_c} \bar{p}_n \boldsymbol{n} \cdot \delta \boldsymbol{g} \, \mathrm{d}S + \int_{\Gamma_c} (-\bar{p}_{tj} \delta \xi^j) \, \mathrm{d}S, \tag{13}$$

$$\int_{\Gamma_c} \delta \bar{p}_n \cdot g \, \mathrm{d}S = 0, \tag{14}$$

where Ω and Γ denote the volume and the surface domain before deformation, respectively. $\rho_0 \boldsymbol{g}$ and $\bar{\boldsymbol{t}}$ are the nominal body force and the traction imposed on Ω and Γ. $\boldsymbol{S}$ and $\boldsymbol{E}$ represent the second Piola–Kirchhoff stress and the Green–Lagrange strain tensors referred to the configuration before deformation. $\bar{p}_n$ and $\bar{p}_{tj}$ are the components of the nominal contact and friction forces. In the case of applying the Lagrange multiplier method to the contact constraint, the contact force $\bar{p}_n$ corresponds to the Lagrange multiplier and is an independent variable. The notation "-", denoting a nominal value, will be omitted hereafter for the sake of brevity.

In this section, the finite element discretization of virtual work due to friction force is introduced. The discretizations of the virtual work due to internal force, external load and contact force are described in [3] and [8]. Instead of a continuous contact surface, the discretized contact model shown in Fig. 2 is considered. The hitting node is assumed to come into contact with the target point. The coordinates and displacements of the target point can be interpolated from nodal values of a target element having m nodes. By denoting the shape function as N_k $(k = 1, m)$ and using the matrix

$$[M] = \begin{bmatrix} -1 & 0 & 0 & N_1 & 0 & 0 & \cdots & N_m & 0 & 0 \\ 0 & -1 & 0 & 0 & N_1 & 0 & \cdots & 0 & N_m & 0 \\ 0 & 0 & -1 & 0 & 0 & N_1 & \cdots & 0 & 0 & N_m \end{bmatrix}, \tag{15}$$

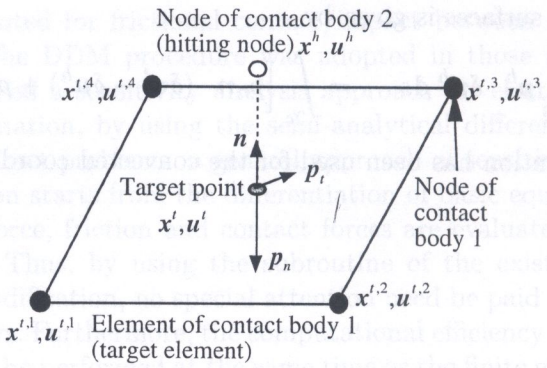

Fig. 2. Discretized contact area

the following relations are obtained:

$$\delta \boldsymbol{u}^t - \delta \boldsymbol{u}^h = [M]\{\delta u\}, \tag{16}$$

$$g = \left(\boldsymbol{x}^t - \boldsymbol{x}^h\right) \cdot \boldsymbol{n} = \{n\}^T [M]\{x\}, \tag{17}$$

where $\{\delta u\}$ and $\{x\}$ consist of virtual nodal displacements and coordinates of the hitting node and the nodes of the target element, namely,

$$\{\delta u\}^T = \left\{\delta u_1^h, \delta u_2^h, \delta u_3^h, \delta u_1^{t,1}, \delta u_2^{t,1}, \delta u_3^{t,1}, \cdots, \delta u_1^{t,m}, \delta u_2^{t,m}, \delta u_3^{t,m}\right\}, \tag{18}$$

$$\{x\}^T = \left\{x_1^h, x_2^h, x_3^h, x_1^{t,1}, x_2^{t,1}, x_3^{t,1}, \cdots, x_1^{t,m}, x_2^{t,m}, x_3^{t,m}\right\}. \tag{19}$$

In the same way, the discretization of kinematic relations can be obtained. For example, by solving Eq. (11), the variation of the convected coordinates of the target point is given in the form

$$\delta \xi^j = \{\delta u\}^T \{\psi_j\}, \tag{20}$$

where $\{\psi_j\}$ is a function of $\{x\}$, $[M]$ and the differentiation of $[M]$ with respect to convected coordinates. On the other hand, the virtual work due to friction force is integrated numerically by taking hitting nodes as integration points of the contact element, i.e.,

$$w_{cf} = \sum_{k=1}^{l} \left(-p_{tj} \delta \xi^j\right)_k w_k J_k, \tag{21}$$

where l is the number of nodes per contact element, and w_k and J_k represent the weight and the Jacobian at the kth node, respectively. Substituting Eq. (20) into Eq. (21) yields

$$w_{cf} = \sum_{k=1}^{l} \{\delta u\}_k^T \left(-p_{tj} \{\psi_j\}\right)_k w_k J_k \tag{22}$$

which gives the discretized form of the fourth term on the right-hand side of Eq. (13) for a contact element. Thus the equivalent nodal friction force of the kth node becomes

$$\{f_t\}_k = \left(-p_{tj} \{\psi_j\}\right)_k w_k J_k. \tag{23}$$

Furthermore, the assemblage for all contact elements, denoted by $\sum_e$, leads to the total equivalent nodal friction force:

$$\boldsymbol{F}_{cf} = \sum_e \sum_{k=1}^{l} \left(-p_{tj} \{\psi_j\}\right)_k w_k J_k. \tag{24}$$

Finally, the discretized equilibrium equation and constraint condition can be given by

$$\boldsymbol{Q} = \boldsymbol{F}_e + \boldsymbol{F}_c + \boldsymbol{F}_{cf}\,, \tag{25}$$

$$\boldsymbol{G} = \boldsymbol{0}, \tag{26}$$

where $\boldsymbol{Q}$, $\boldsymbol{F}_e$, $\boldsymbol{F}_c$ and $\boldsymbol{F}_{cf}$ represent the total nodal internal force, the external load, and the contact and friction forces, respectively. $\boldsymbol{G}$ denotes the nodal penetration assembled for the whole contact surface.

2.2. Sensitivity analysis for frictional contact problems

In this section, the formulation is first performed on the continuum base for generality and then the discretized form is derived. By introducing notations of W_i and W_e for the virtual work due to internal force and external load, as well as W_c and W_{cf} for the virtual work due to contact and friction forces, respectively, the virtual work equation (Eq. (13)) and constraint condition (Eq. (14)) for the whole structure are written as

$$W_i(\boldsymbol{u}, \boldsymbol{b}) = W_e + W_c(\boldsymbol{u}, p_n, \boldsymbol{b}) + W_{cf}(\boldsymbol{u}, p_n, \boldsymbol{b})\,, \tag{27}$$

$$G(\boldsymbol{u}, \boldsymbol{b}) \;\; = 0. \tag{28}$$

For brevity, the external load is assumed to be independent of design parameters. From the viewpoint of the physical mechanism and mathematical treatment, the penalty constraint is introduced for the stick state, i.e., a small slip is allowed and the friction force depends on the displacement and contact force (see, for example, [6]). The contact force p_n is an independent variable, in addition to displacement $\boldsymbol{u}$, as mentioned before. $\boldsymbol{b}$ denotes a vector with design parameters as its components. The effect of design parameters on the virtual work can be classified into two parts. The first part depends explicitly on the variation of the design parameters and can be obtained analytically. On the other hand, the second part is caused by the variation of structural responses $\boldsymbol{u}$ and p_n, which depends implicitly on the design parameters and, in general, cannot be determined directly. The evaluation of the latter is the key point in sensitivity analysis.

In this work, the partial variations of a specified variable with respect to displacement, contact force and design parameter are denoted by $\partial_u[\bullet]$, $\partial_{p_n}[\bullet]$ and $\partial_b[\bullet]$, respectively. Thus, the variations of Eqs. (27) and (28) with respect to design parameters are given by

$$\partial_u[W_i] - (\partial_u[W_c] + \partial_{p_n}[W_c]) - (\partial_u[W_{cf}] + \partial_{p_n}[W_{cf}]) + (\partial_b[W_i] - \partial_b[W_c] - \partial_b[W_{cf}]) = 0\,, \tag{29}$$

$$\partial_u[G] + \partial_b[G] = 0. \tag{30}$$

The evaluations of the terms related to internal and contact forces and constraint condition are discussed in [4], and only the variation due to friction is considered here. Since the integrals in the virtual work equation depends on the design shape, for the convenience of treating the design shape as a design parameter, an invertible mapping is introduced in such a way that the fixed domain ∇_c is the image of contact area Γ_c under the mapping. A convected coordinate system is suitable for this purpose. According to this mapping and taking design parameters into account, the virtual work due to friction force, i.e., the last term on the right-hand side of Eq. (13), becomes

$$W_{cf} = \int_{\nabla_c} -p_{tj}(\boldsymbol{u}, p_n, \boldsymbol{b})\, \delta\xi^j(\boldsymbol{u}, \boldsymbol{b})\, J(\boldsymbol{b})\, \mathrm{d}\xi^1 \mathrm{d}\xi^2. \tag{31}$$

As a function of design parameter, the Jacobian $J(\boldsymbol{b})$ of the mapping reflects the dependence on the design shape. Since the integration domain is now independent of the design parameter, only the variations of the integrand with respect to the design parameter should be considered. By denoting

the total variation of a specified variable as $D[\bullet]$ and the partial variation due to displacement and contact force as $\tilde{D}[\bullet]$, i.e.,

$$D[\bullet] = \partial_u[\bullet] + \partial_{p_n}[\bullet] + \partial_b[\bullet] \tag{32}$$

$$\tilde{D}[\bullet] = \partial_u[\bullet] + \partial_{p_n}[\bullet], \tag{33}$$

the variation of Eq. (31) can be expressed as

$$D[W_{cf}] = \tilde{D}[W_{cf}] + \partial_b[W_{cf}], \tag{34}$$

where

$$\tilde{D}[W_{cf}] = \int_{\nabla_c} \tilde{D}\left[-p_{tj}(\boldsymbol{u}, p_n, \boldsymbol{b})\,\delta\xi^j(\boldsymbol{u}, \boldsymbol{b})\right] J(\boldsymbol{b})\,\mathrm{d}\xi^1\mathrm{d}\xi^2\,, \tag{35}$$

$$\begin{aligned}\partial_b[W_{cf}] &= \int_{\nabla_c} \partial_b\left[-p_{tj}(\boldsymbol{u}, p_n, \boldsymbol{b})\,\delta\xi^j(\boldsymbol{u}, \boldsymbol{b})J(\boldsymbol{b})\right]\,\mathrm{d}\xi^1\mathrm{d}\xi^2 \\ &= \int_{\nabla_c} \partial_b\left[-p_{tj}(\boldsymbol{u}, p_n, \boldsymbol{b})\right]\,\delta\xi^j(\boldsymbol{u}, \boldsymbol{b})J(\boldsymbol{b})\,\mathrm{d}\xi^1\mathrm{d}\xi^2 \\ &\quad + \int_{\nabla_c} -p_{tj}(\boldsymbol{u}, p_n, \boldsymbol{b})\,\partial_b\left[\delta\xi^j(\boldsymbol{u}, \boldsymbol{b})J(\boldsymbol{b})\right]\,\mathrm{d}\xi^1\mathrm{d}\xi^2.\end{aligned} \tag{36}$$

It is noted that Eq. (35) is equivalent to the linearized form of the virtual work due to friction force, and thus results in the frictional tangent stiffness, as shown later. The second term on the right-hand side of Eq. (36) can be calculated explicitly, or it will vanish when shape is not taken to be a design parameter. On the other hand, the first term represents the variation due to design parameters while displacement and contact force remain the same as those of the original structure, in which the design parameter is set to be the design value. The calculation of this term must be carried out in accordance with the adopted friction law and the discretization in the specified finite element analysis.

The assemblage of Eq. (21) for the whole contact surface and the use of Eq. (20) lead to the discretized form of the virtual work due to friction force, namely,

$$W_{cf} = \sum_e \sum_{k=1}^{l} \{\delta u\}_k^T \left(-p_{tj}\{\psi_j\}\right)_k w_k J_k\,. \tag{37}$$

Thus, the discretization of Eqs. (35) and (36) gives

$$\tilde{D}[W_{cf}] = \sum_e \sum_{k=1}^{l} \{\delta u\}_k^T\, \tilde{D}\left[\left(-p_{tj}\{\psi_j\}\right)_k\right] w_k J_k\,, \tag{38}$$

$$\partial_b[W_{cf}] = \sum_e \sum_{k=1}^{l} \{\delta u\}_k^T\, \partial_b\left[\left(-p_{tj}\{\psi_j\}\right)_k w_k J_k\right], \tag{39}$$

where the notations of arguments are omitted. For the friction law with a penalty constraint for the stick state, the friction force depends on displacement and contact force. Therefore, the variation of friction force due to displacement and contact force can be expressed as

$$\tilde{D}[(-p_{tj})_k] = \left\{\{\phi_j\}^T, \omega_j\right\}_k \left\{\begin{array}{c}\{\mathrm{d}u\} \\ \mathrm{d}p_n\end{array}\right\}_k. \tag{40}$$

Also, by taking a variation of Eq. (11), we can obtain

$$\tilde{D}[(\delta\xi^j)_k] = \{\delta u\}_k^T [\Psi_j]_k \{\mathrm{d}u\}_k\,, \tag{41}$$

where the detailed calculation is omitted. The variables $\{\psi_j\}$, $\{\phi_j\}$, ω_j and $[\Psi_j]$ are evaluated from nodal coordinates, displacements and contact forces of the original structure together with the shape function and friction coefficient. Finally, the total variation of Eq. (37) is given by

$$\begin{aligned} D[W_{cf}] &= \tilde{D}[W_{cf}] + \partial_b[W_{cf}] \\ &= \{\delta \boldsymbol{U}^T, \delta \boldsymbol{P}_n^T\} [\boldsymbol{K}_{cf}] \begin{Bmatrix} \mathrm{d}\boldsymbol{U} \\ \mathrm{d}\boldsymbol{P}_n \end{Bmatrix} + \{\delta \boldsymbol{U}^T, \delta \boldsymbol{P}_n^T\} \begin{Bmatrix} \partial_b [\boldsymbol{F}_{cf}] \\ \boldsymbol{0} \end{Bmatrix}, \end{aligned} \tag{42}$$

where

$$\begin{aligned} [\boldsymbol{K}_{cf}] \quad = \sum_e \sum_{k=1}^{l} \Bigg\{ \Bigg(\begin{bmatrix} \{\psi_1\}\{\phi_1\}^T & \{\psi_1\}\omega_1 \\ \{0\}^T & 0 \end{bmatrix} + \begin{bmatrix} -p_{t1}[\Psi_1] & \{0\} \\ \{0\}^T & 0 \end{bmatrix} \\ + \begin{bmatrix} \{\psi_2\}\{\phi_2\}^T & \{\psi_2\}\omega_2 \\ \{0\}^T & 0 \end{bmatrix} + \begin{bmatrix} -p_{t2}[\Psi_2] & \{0\} \\ \{0\}^T & 0 \end{bmatrix} \Bigg)_k w_k J_k \Bigg\}. \end{aligned} \tag{43}$$

$$\partial_b[\boldsymbol{F}_{cf}] = \partial_b \left[\sum_e \sum_{k=1}^{l} \left(-p_{tj}\{\psi_j\}\right)_k w_k J_k \right]. \tag{44}$$

It is clear that $[\boldsymbol{K}_{cf}]$ is identical to the frictional tangent stiffness in the finite element analysis. $\mathrm{d}\boldsymbol{U}$ and $\mathrm{d}\boldsymbol{P}_n$ are the total variations, i.e., sensitivities, of the nodal displacement and contact force with respect to design parameters. Furthermore, by using Eq. (24) in (37) and considering the arbitrariness of virtual displacement and contact force, the variation of nodal friction force with respect to design parameter is given by

$$D[\boldsymbol{F}_{cf}] = [\boldsymbol{K}_{cf}] \begin{Bmatrix} \mathrm{d}\boldsymbol{U} \\ \mathrm{d}\boldsymbol{P}_n \end{Bmatrix} + \begin{Bmatrix} \partial_b[\boldsymbol{F}_{cf}] \\ \boldsymbol{0} \end{Bmatrix}. \tag{45}$$

Although, in principle, the variation $\partial_b[\boldsymbol{F}_{cf}]$ may be evaluated analytically, the formulation is complicated in general. Also, the formulation and implementation must be carried out each time for different element types and friction laws adopted in the finite element analysis.

In this work, an alternative approach is taken as follows. For an original structure in an equilibrium state, displacement and contact force fields are determined based on design values of design parameters. Assuming a perturbed structure in which the design parameters are perturbed while the displacement and contact force are kept the same as those of the original structure, unbalance force would occur. It is noted that $\partial_b[\boldsymbol{F}_{cf}]$ represents the variational form of the unbalance of the friction force. On the other hand, if the finite perturbation of design parameter $\Delta \boldsymbol{b}$ is small, as a first-order approximation, the variation can be written as

$$\partial_b[\boldsymbol{F}_{cf}] \approx \frac{\partial \boldsymbol{F}_{cf}}{\partial \boldsymbol{b}} \cdot \Delta \boldsymbol{b} \equiv \Delta_b[\boldsymbol{F}_{cf}]. \tag{46}$$

It is noted that $\Delta_b[\boldsymbol{F}_{cf}]$ gives the finite difference form of the unbalance force due to friction. This implies that the variation in friction force may be evaluated numerically from the difference between friction forces of the original and perturbed structures. Thus, the use of the displacement and the contact force of the original structure, which are obtained in finite element analysis, together with the design value $\boldsymbol{b}_o$ and the perturbed value $\boldsymbol{b}_o + \Delta \boldsymbol{b}$ of the design parameter in Eq. (23) leads to

$$\begin{aligned} \partial_b[\{f_t\}_k] &\approx \Delta_b[\{f_t\}_k] \\ &= \left(-p_{tj}(\boldsymbol{u}_o, p_{n,o}, \boldsymbol{b}_o + \Delta \boldsymbol{b})\{\psi_j(\boldsymbol{u}_o, \boldsymbol{b}_o + \Delta \boldsymbol{b})\}\right)_k w_k J_k(\boldsymbol{b}_o + \Delta \boldsymbol{b}) \\ &\quad - \left(-p_{tj}(\boldsymbol{u}_o, p_{n,o}, \boldsymbol{b}_o)\{\psi_j(\boldsymbol{u}_o, \boldsymbol{b}_o)\}\right)_k w_k J_k(\boldsymbol{b}_o), \end{aligned} \tag{47}$$

where the subscript "o" denotes the value in the original structure. By assembling for all contact elements, the variation of total nodal friction force is given by

$$\partial_b[\boldsymbol{F}_{cf}] \approx \Delta_b[\boldsymbol{F}_{cf}] = \sum_e \sum_{k=1}^{l} \Delta_b\left[\{f_t\}_k\right]. \tag{48}$$

The subroutine of computing the friction force in the finite element analysis code can be used directly for the evaluation of Eqs. (47) and (48). This means that the existing finite element analysis code may be easily extended to carry out the sensitivity analysis without paying special attention, in the sensitivity analysis stage, to the adopted element type or friction law.

The variation of the equilibrium equation (25) and constraint condition (26) gives

$$D[\boldsymbol{Q}] = D[\boldsymbol{F}_c] + D[\boldsymbol{F}_{cf}], \tag{49}$$

$$D[\boldsymbol{G}] = \boldsymbol{0}, \tag{50}$$

and, furthermore, results in

$$D[\boldsymbol{Q}] \quad = \partial_u[\boldsymbol{Q}] + \partial_b[\boldsymbol{Q}] = \boldsymbol{K}_i \mathrm{d}\boldsymbol{U} + \partial_b[\boldsymbol{Q}], \tag{51}$$

$$\begin{Bmatrix} D[\boldsymbol{F}_c] \\ \partial_u[\boldsymbol{G}] \end{Bmatrix} = \begin{Bmatrix} \partial_u[\boldsymbol{F}_c] + \partial_{p_n}[\boldsymbol{F}_c] + \partial_b[\boldsymbol{F}_c] \\ -\partial_b[\boldsymbol{G}] \end{Bmatrix} = \boldsymbol{K}_c \begin{Bmatrix} \mathrm{d}\boldsymbol{U} \\ \mathrm{d}\boldsymbol{P}_n \end{Bmatrix} + \begin{Bmatrix} \partial_b[\boldsymbol{F}_c] \\ -\partial_b[\boldsymbol{G}] \end{Bmatrix}, \tag{52}$$

where $\boldsymbol{K}_i$ and $\boldsymbol{K}_c$ represent tangent stiffness due to internal and contact forces. $\partial_b[\boldsymbol{Q}]$, $\partial_b[\boldsymbol{F}_c]$ and $\partial_b[\boldsymbol{G}]$ are also approximately evaluated in the following forms [4]:

$$\partial_b[\boldsymbol{Q}] \approx \Delta_b[\boldsymbol{Q}] = \boldsymbol{Q}(\boldsymbol{U}_o, \boldsymbol{b}_o + \Delta\boldsymbol{b}) - \boldsymbol{Q}(\boldsymbol{U}_o, \boldsymbol{b}_o), \tag{53}$$

$$\partial_b[\boldsymbol{F}_c] \approx \Delta_b[\boldsymbol{F}_c] = \boldsymbol{F}_c(\boldsymbol{U}_o, \boldsymbol{P}_{n,o}, \boldsymbol{b}_o + \Delta\boldsymbol{b}) - \boldsymbol{F}_c(\boldsymbol{U}_o, \boldsymbol{P}_{n,o}, \boldsymbol{b}_o), \tag{54}$$

$$\partial_b[\boldsymbol{G}] \approx \Delta_b[\boldsymbol{G}] = \boldsymbol{G}(\boldsymbol{U}_o, \boldsymbol{b}_o + \Delta\boldsymbol{b}) - \boldsymbol{G}(\boldsymbol{U}_o, \boldsymbol{b}_o). \tag{55}$$

Finally, by substituting Eqs. (45), (51) and (52) into Eqs. (49) and (50), and using Eqs. (48), (53)–(55), the sensitivities of nodal displacement and contact force are given by

$$\begin{Bmatrix} \mathrm{d}\boldsymbol{U}/\mathrm{d}\boldsymbol{b} \\ \mathrm{d}\boldsymbol{P}_n/\mathrm{d}\boldsymbol{b} \end{Bmatrix} \approx \boldsymbol{K}^{-1} \begin{Bmatrix} \left(-\Delta_b[\boldsymbol{Q}] + \Delta_b[\boldsymbol{F}_c] + \Delta_b[\boldsymbol{F}_{cf}]\right)/\Delta\boldsymbol{b} \\ -\Delta_b[\boldsymbol{G}]/\Delta\boldsymbol{b} \end{Bmatrix}, \tag{56}$$

where

$$\boldsymbol{K} = \begin{bmatrix} \boldsymbol{K}_i & \boldsymbol{0} \\ \boldsymbol{0} & \boldsymbol{0} \end{bmatrix} - [\boldsymbol{K}_c] - [\boldsymbol{K}_{cf}] \tag{57}$$

is the tangent stiffness for the whole structure. Once the iterative computation of the finite element analysis converges, the forward decomposed tangent stiffness matrix, which is denoted as $\boldsymbol{K}^{-1}$, can be utilized for the sensitivity analysis. Thus, the sensitivities are computed from Eq. (56) without iteration. Since the construction of the tangent stiffness and its triangular decomposition are time-consuming, excluding these procedures from the sensitivity analysis stage results in a high computational efficiency for large-scale nonlinear problems.

3. Numerical examples

The sensitivity analysis approach proposed in Sec. 2 is implemented into a finite element analysis code [6] developed by the authors for elastoplastic frictional contact problems with large deformation. The Coulomb friction law similar to the constitutive relationship of elastoplasticity is used, i.e., small slip is allowed even in the stick state. Numerical examples are carried out using a hexahedral type of element with eight nodes to assess the proposed algorithm. In sensitivity analysis, the design parameter b is normalized as $b = b_o(1 + \beta_b)$, where b_o denotes the design value.

3.1. Indentation of a rigid body into elastic foundation

In the first example, attention is focused on the sensitivity analysis of frictional contact behavior, thus, small deformation and elasticity are assumed. The distribution of contact pressure and its sensitivity with respect to the friction coefficient μ are computed for the finite element model shown in Fig. 3.

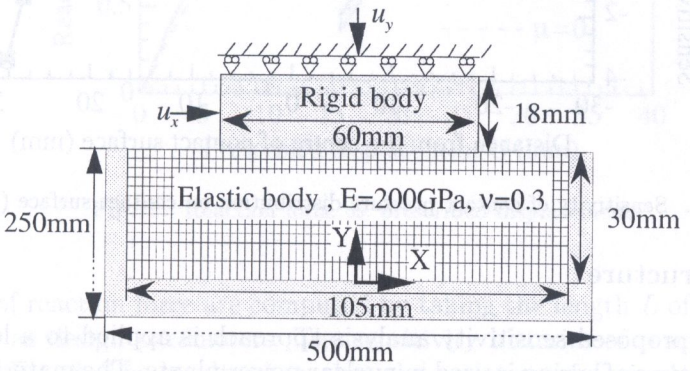

Fig. 3. Indentation of a rigid body into elastic body

The degree of freedom in the direction out of the plane is constrained to simulate a 2-D problem. The fine mesh, as shown in Fig. 3, is used to obtain a smooth distribution of pressure, but a rough mesh, with dimensions of 500 mm × 250 mm, is connected to the fine part to approximate a half-infinite body. Displacement is specified to be $u_x = 3.33\,\text{mm}$ and $u_y = -0.01\,\text{mm}$, for a width of 1.67 mm for an element, such that finite sliding is generated. The results of contact pressure are shown in Fig. 4. The gradient of pressure is sharp on both sides and the larger gradient is observed on the left side. This result is considered to be due to the reaction force of the rigid body, which resists the moment resulting from friction. The distribution of the sensitivity of contact pressure shown in Fig. 5 confirms that such a trend will become considerable when the friction coefficient increases. For comparison, the results of contact pressure and its sensitivity obtained by the general code, MARC, using the FDM are also shown in Figs. 4 and 5, respectively. The results agree well with the present work.

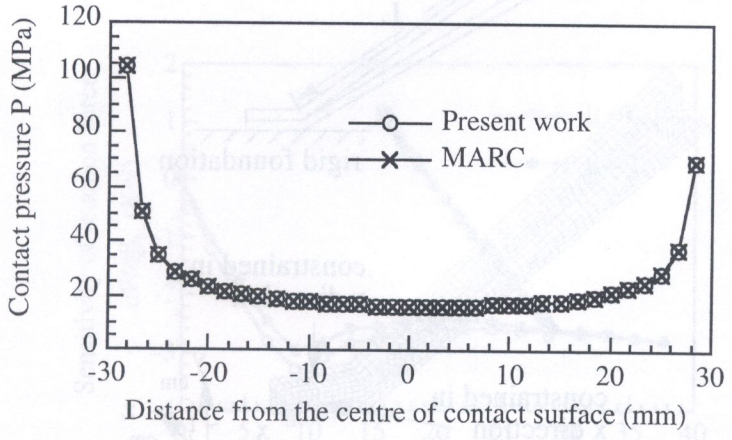

Fig. 4. Contact pressure distribution on contact surface ($\mu = 0.5$)

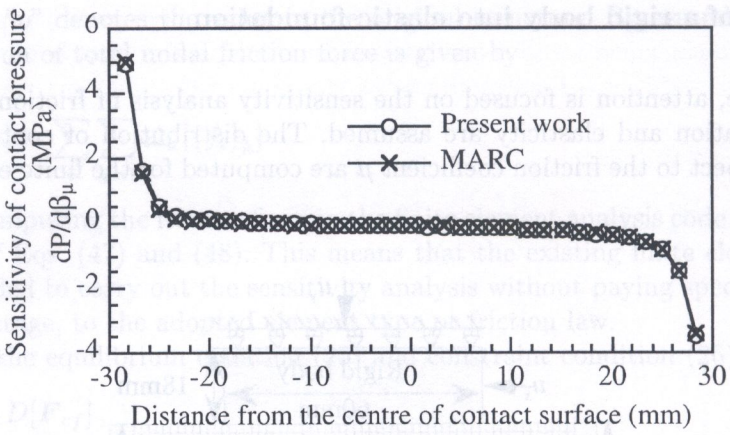

Fig. 5. Sensitivity of contact pressure distribution on contact surface ($\mu = 0.5$)

3.2. Leaf spring structure

In this example, the proposed sensitivity analysis approach is applied to a leaf spring structure as shown in Fig. 6. This type of spring is used in nuclear power plants. The material property is modeled by elastoplasticity with the associated flow rule of von Mises type and isotropic work hardening. The stress is updated incrementally by the radial return algorithm. The prescribed displacement is given by pushing a rigid block on the tip of the upper spring. Frictional contact is considered between the two leaves, and also between the upper leaf and the rigid body. The same friction coefficient is assumed at both interfaces. Due to symmetry, only half of the structure is modeled and computed.

The reaction forces of the spring to the rigid body with friction coefficients $\mu = 0.0$ and $\mu = 0.5$ are shown in Fig. 7. It is noted that the existence of friction results in another load path dependency of structural response besides that by elastoplasticity. The strain energy stored by the friction force causes a larger reaction force than that in the frictionless case. Right after unloading, the reversed friction force releases the strain energy and leads to a sharp drop in the reaction force. The reverse situation occurs during the reloading process.

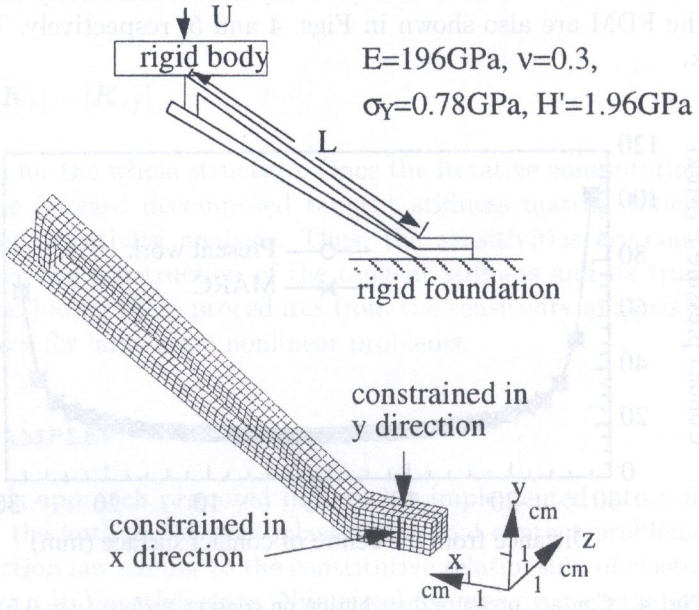

Fig. 6. Leaf spring loaded by rigid body

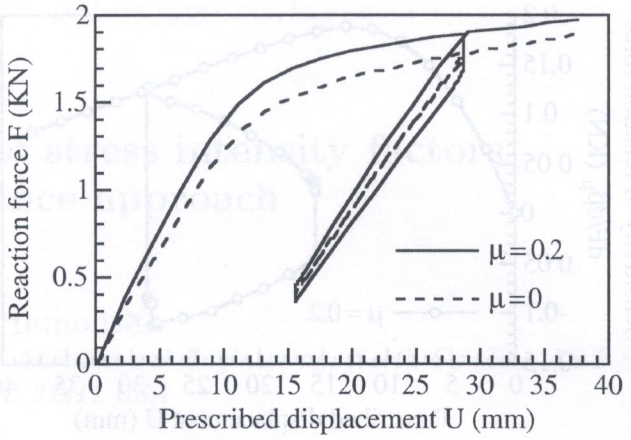

Fig. 7. Reaction force *vs.* prescribed displacement

The sensitivities of reaction force are computed by taking the length L of the upper leaf and the friction coefficient μ as design parameters. The sensitivity histories of reaction force with respect to L are depicted in Fig. 8. The results show that the variation of L similarly affects the reaction forces in both frictional and frictionless cases. On the other hand, Fig. 9 shows the sensitivity history of reaction force with respect to friction coefficient μ. A significant path dependency of the sensitivity history due to friction is observed. Although the sensitivity of reaction force with respect to the friction coefficient is one order less than that with respect to the length L, taking the uncertainty of the friction coefficient into account, this influence should not be neglected in engineering applications. The sensitivity results are compared with those obtained from FDM and good agreement is obtained.

Since the proposed semi-analytical approach is characterized by numerical evaluation of the variations in contact and friction forces with respect to design parameters, the influence of the perturbation specified for a design parameter on the accuracy must be investigated. It is confirmed that stable and accurate sensitivity results can be obtained for dimensionless variables β_L and β_μ varying from 10^{-3} to 10^{-9}. The CPU time of the finite element analysis was about 615 minutes. On the other hand, the sensitivity analysis took a CPU time of only about 18 minutes per design parameter. The computational efficiency of the proposed approach is clearly superior to that of FDM in which an additional finite element analysis must be carried out per design parameter to obtain the sensitivity.

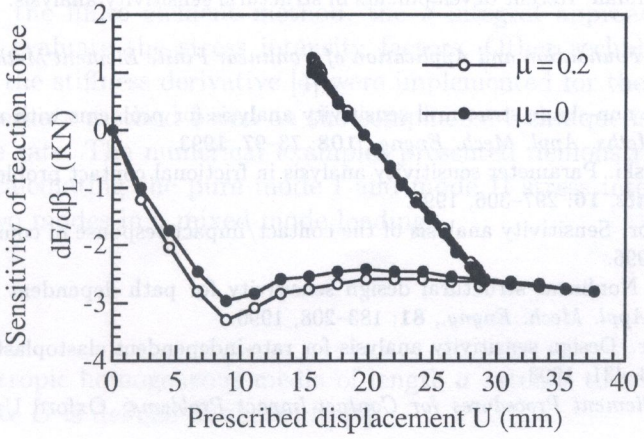

Fig. 8. Sensitivity histories of reaction force with respect to L

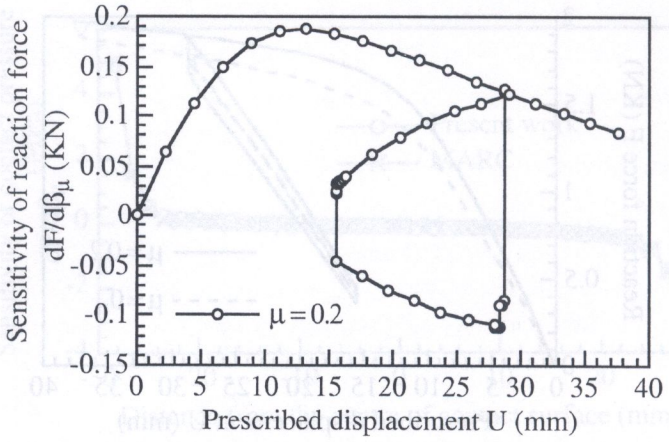

Fig. 9. Sensitivity history of reaction force with respect to μ

4. Conclusions

In this work, a practical approach for the sensitivity analysis of frictional contact problems was proposed. The formulations are based on the direct differentiation method but the variations in friction force with respect to the design parameters are evaluated numerically. Thus the computational efficiency of the direct differentiation method is maintained while generality is achieved in the sense that the approach is not dependent on the specific form of the friction law adopted. Therefore, the sensitivity analysis function can be easily added to the existing finite element analysis code. Through two numerical examples, the efficiency of the proposed approach was verified.

References

[1] H.J. Antúnez, M. Kleiber. Parameter sensitivity of metal forming processes. *Computer Assisted Mechanics and Engineering Sciences*, **3**: 263–282, 1996.

[2] H.J. Antúnez, M. Kleiber. Sensitivity analysis of metal forming processes involving frictional contact in steady state. *J. Materials Processing Technology*, **60**: 485–491, 1996.

[3] K.-J. Bathe. *Finite Element Procedures.* Prentice Hall, 1996.

[4] X. Chen. Nonlinear finite element sensitivity analysis for large deformation elastoplastic and contact problems. Ph.D. dissertation. The University of Tokyo, Japan, 1994.

[5] X. Chen, M. Mori, T. Hisada. A sensitivity analysis for frictionless contact problems. *Computer Assisted Mechanics and Engineering Sciences*, **3**: 403–423, 1996.

[6] X. Chen, K. Nakamura, M. Mori, T. Hisada. Finite element analysis for multi-leaf structures with frictional contact and large deformation. *Computer Assisted Mechanics and Engineering Sciences*, **7**: 53–67, 2000.

[7] R.T. Haftka, H.M. Adelman. Recent developments in structural sensitivity analysis. *Struct. Optim.*, **1**: 137–151, 1989.

[8] T. Hisada, H. Noguchi. *Foundation and Application of Nonlinear Finite Element Method* (in Japanese). Maruzen, Tokyo, 1995.

[9] M. Kleiber. Shape and non-shape structural sensitivity analysis for problems with any material and kinematic non-linearity. *Comp. Meths. Appl. Mech. Engng.*, **108**: 73–97, 1993.

[10] M. Kleiber, W. Sosnowski. Parameter sensitivity analysis in frictional contact problems of sheet metal forming. *Computational Mechanics*, **16**: 297–306, 1995.

[11] G.D. Pollock, A.K. Noor. Sensitivity analysis of the contact/impact response of composite structures. *Comput. Struct.*, **61**: 251–269, 1996.

[12] J.J. Tsay, J.S. Arora. Nonlinear structural design sensitivity for path dependent problems. Part 1: General theory. *Comp. Meths. Appl. Mech. Engng.*, **81**: 183–208, 1990.

[13] C.A. Vidal, R.B. Haber. Design sensitivity analysis for rate-independent elastoplasticity. *Comp. Meths. Appl. Mech. Engng.*, **107**: 393–431, 1993.

[14] Z.-H. Zhong. *Finite Element Procedures for Contact-Impact Problems.* Oxford University Press, New York, 1993.

[15] Z.-H. Zhong, J. Mackerle. Static contact problems – a review. *Engineering Computations*, **9**: 3–37, 1992.